Use of 2-pyrimidineamidoxime to generate polynuclear homo-/heterometallic assemblies: synthesis, crystal structures and magnetic study with theoretical investigations on the exchange mechanism†

Bappaditya Gole,[a] Rajesh Chakrabarty,[a] Sandip Mukherjee,[a] You Song[b] and Partha Sarathi Mukherjee*[a]

Received 21st April 2010, Accepted 22nd July 2010
DOI: 10.1039/c0dt00353k

Three new transition metal complexes using 2-pyrimidineamidoxime ($pmadH_2$) as multidentate chelating and/or bridging ligand have been synthesized and characterized. The ligand $pmadH_2$ has two potential bridging functional groups [μ-O and μ-(N–O)] and consequently shows several coordination modes. While a polymeric 1D Cu^{II} complex $[Cu(pmadH_2)_2(NO_3)](NO_3)$ (**1**) was obtained upon treatment of $Cu(NO_3)_2{\cdot}3H_2O$ with $pmadH_2$ at room temperature in the absence of base, a high temperature reaction in the presence of base yielded a tetranuclear Cu^{II}-complex $[Cu_4(pmad)_2(pmadH)_2(NO_3)](NO_3)(H_2O)$ (**2**). One of the Cu^{II} centers is in a square pyramidal environment while the other three are in a square planar geometry. Reaction of the same ligand with an equimolar mixture of both $Cu(NO_3)_2{\cdot}3H_2O$ and $NiCl_2{\cdot}6H_2O$ yielded a tetranuclear heterometallic $Cu^{II}_2Ni^{II}_2$ complex $[Cu_2Ni_2(pmad)_2(pmadH)_2Cl_2]{\cdot}H_2O$ (**3**) containing both square planar (Ni^{II}) and square pyramidal (Cu^{II}) metal centers. Complexes **1–3** represent the first examples of polynuclear metal complexes of 2-pyrimidineamidoxime. The analysis of variable temperature magnetic susceptibility data of **2** reveals that both ferromagnetic and antiferromagnetic interactions exist in this complex ($J_1 = +10.7$ cm^{-1} and $J_2 = -2.7$ cm^{-1} with $g = 2.1$) leading to a resultant ferromagnetic behavior. Complex **3** shows expected antiferromagnetic interaction between two Cu^{II} centers through –N–O– bridging pathway with $J_1 = -3.4$ cm^{-1} and $g = 2.08$. DFT calculations have been used to corroborate the magnetic results.

Introduction

Ever since the first report of a metallacrown (MC) [9-MC-3] in 1989 by Pecoraro and his co-workers,[1] metallacrowns have emerged as a special class of compounds in coordination chemistry.[1,2] These compounds have received considerable attention in recent years not only for their diverse architectures but also for their potential applications in host–guest chemistry,[3] recognition reagents,[4] catalysis,[5] sensors,[6] bioactivities,[7] chiral motifs for 2D and 3D solids,[8] single-molecule magnets (SMMs) and single-chain magnets (SCMs).[9]

These compounds are broadly divided into two categories: (a) Metallacrowns with $[M–N–O]_n$ repeating units synthesized using multidentate ligands such as hydroxamic,[10] ketonoxime,[11] and aminohydroxamic acids[12] with varying ring sizes ranging from 9-MC-3 to 24-MC-8.[13] This class also includes inverse metallacrowns.[14] (b) Metallacrowns with the $[M–N–N]_n$ repeating linkage, better known as azametallacrowns, that are synthesized utilizing multidentate ligands such as *N*-substituted salicylhydrazide, salicylhydrazone, or 2-pyridinecarbaldehyde hydrazone. Their ring size ranges from 18-MC-6 to 60-MC-16.[15]

For 12-MC-4 complexes, which are relevant to the present discussion, two different linkages have been reported: classical or regular[16] and the less common inverse.[15] In the classical motif, there is a N–O–M–N–O–M linkage, *i.e.*, a $[M–N–O]_n$ repeat unit, with the oxygen atoms pointing towards the centre of the cavity, suitable for binding cations. However, the inverse motif, with the linkage N–O–M–O–N–M has only been realized for Zn[15] and Co ions,[17] with the ring metal ions oriented towards the centre of the cavity suitable for encapsulating anions. Collapsed MCs contain no central guest metal atoms, but instead of retaining the vacant cavity, the ring oxygens of the MC bind to ring metal ions on the opposite side of the MC ring. Several collapsed 12-MC-4 complexes have been reported with oxime based ligands. All of the complexes contain a nearly planar M^{II}_4 core.[18]

The oxime ligands have been extensively used in the synthesis of 3d transition metal clusters.[10] The monoanionic 2-pyridylaldoxime/ketoximes, (py)C(R)NOH (R = H, Me, Ph, *etc.*), are well known to form homo- and heterometallic clusters with fascinating structures and magnetic properties.[10,19] The coordination chemistry of analogous organic molecules, in which the non-donor R group is replaced by a donor group (hydroxy in the case of the oxamic acids and amino for the amidoximes), have also recently been explored. In this series of ligands 2-pyridineamidoxime was shown to form a dodecanuclear Ni^{II} cluster.[20] We were interested in investigating the effect of an added nitrogen atom in the aromatic ring at a suitable coordinating site along with the ionisable amino group and hence we prepared

[a]*Department of Inorganic and Physical Chemistry, Indian Institute of Science, Bangalore, 560 012, India. E-mail: psm@ipc.iisc.ernet.in; Fax: 91-80-2360-1552; Tel: 91-80-2293-3352*
[b]*State Key Laboratory of Coordination Chemistry, Nanjing University, Nanjing, 210093, China*

† Electronic supplementary information (ESI) available: X-ray crystallographic data in CIF format, H-bonding parameters, XPS plots and powder XRD pattern of **3**, Curie–Weiss fitting of the χ_M^{-1} *vs.* *T* data and atomic spin densities of **2** and **3**. CCDC reference numbers 774587–774589. For ESI and crystallographic data in CIF or other electronic format see DOI: 10.1039/c0dt00353k

the ligand 2-pyrimidineamidoxime ($pmadH_2$). Though the added nitrogen did not take part in bonding in any of its complexes reported here, we were able to isolate three new transition metal complexes through optimized synthetic procedures. Herein we report the synthesis and crystal structures of a 1D Cu(II) chain (**1**) and two collapsed metallacrowns (**2** and **3**). The magnetic behavior of these two metallacrowns **2** and **3** corroborate well with the DFT calculations. In these complexes, 2-pyrimidineamidoxime ligand adopts several coordination modes in its neutral and dianionic state (Scheme 1). To the best of our knowledge complexes **1–3** represent the first examples of polynuclear metal complexes of $pmadH_2$.

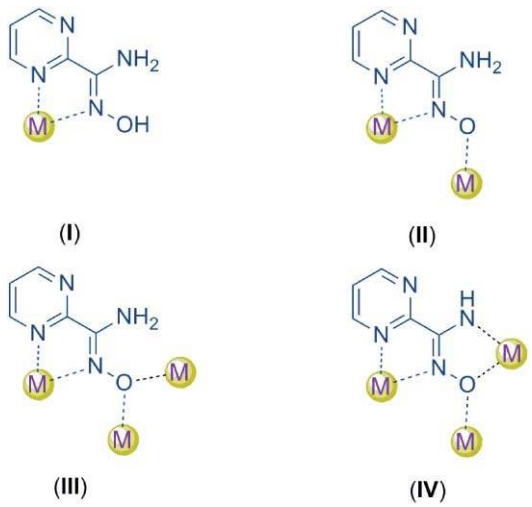

Scheme 1 Observed coordination modes of 2-pyrimidineamidoxime ligand in **1–3**.

Experimental section

Materials and physical measurements

$Cu(NO_3)_2{\cdot}3H_2O$, $NiCl_2{\cdot}6H_2O$, $NH_2OH{\cdot}HCl$, 2-cyanopyrimidine and Na_2CO_3 were obtained from commercial sources and were used as received without further purification. Elemental analyses of C, H, and N were performed using a Perkin-Elmer 240C elemental analyzer. IR spectra were recorded as KBr pellets using a Magna 750 FT-IR spectrophotometer in the range of 4000–400 cm^{-1}. X-ray photoelectron spectroscopy of complex **3** was recorded in a Thermo Fisher Scientific Multilab 2000 (England) with Al–Kα radiation (1486.6 eV). Binding energies reported here are with reference to graphite at 284.5 eV. Samples were mixed with 30% (by weight) of graphite powder to make thin pellets for XPS data collection at room temperature. EPR data were recorded using a Bruker EMX X-band EPR spectrometer (9.40 GHz) at different temperatures. The *g* values were calibrated with diphenylpicrylhydrazyl (DPPH) radical standard. Variable temperature (1.8–300 K) magnetic susceptibility data of the powdered samples were collected using a Quantum Design MPMS-XL5 SQUID magnetometer at an external applied dc field of 0.1 T for **2** and at 0.2 T for **3**. The experimental susceptibility data were corrected for diamagnetism (Pascal's tables).[21]

Synthesis of the ligand $pmadH_2$

The ligand was prepared using a slightly modified method of the reported procedure.[22] $NH_2OH{\cdot}HCl$ (1.39 g, 20 mmol) was neutralized by sodium carbonate (1.06 g, 10 mmol) in water (20 mL) to which 2-cyanopyrimidine (2.10 g, 20 mmol) in 10 mL of ethanol was added dropwise. The resulting mixture was heated to reflux for 2 h and cooled down to room temperature. The ethanol was removed by a rotary evaporator and the final mixture was kept in an ice bath. White crystalline material started to appear after a few minutes. The crystalline material was filtered and washed thoroughly with cold ethanol and dried under vacuum. Isolated yield: 2.48 g (90%).

Synthesis of $[Cu(pmadH_2)_2(NO_3)](NO_3)$ (1)

$Cu(NO_3)_2{\cdot}3H_2O$ (0.5 mmol, 121.0 mg) was dissolved in 10 mL methanol and solid 2-pyrimidineamidoxime (0.5 mmol, 69.0 mg) was added to it in portions. The resulting green solution was stirred for 15 min at room temperature and filtered. The solvent was evaporated to dryness to obtain **1** as green crystalline material. Isolated yield: 41% (based on copper). X-ray diffraction quality crystals were obtained by slow vapor diffusion of diethyl ether into the green filtrate. Anal. Calcd. for **1**, $C_{10}H_{12}N_{10}O_8Cu$: C, 25.90; N, 30.20; H, 2.61. Found: C, 26.16; N, 30.15; H, 2.78. IR (KBr, cm^{-1}): 3415, *ν*(NH); 3236, *ν*(OH); 1683, *ν*(C═N); 1594, 1395, 1305, 1264 and 1031.

Synthesis of $[Cu_4(pmad)_2(pmadH)_2(NO_3)](NO_3)(H_2O)$ (2)

$Cu(NO_3)_2{\cdot}3H_2O$ (0.5 mmol, 121.0 mg) and 2-pyrimidineamidoxime (0.5 mmol, 69.0 mg) were dissolved in a 15 mL 2 : 1 mixture of distilled water and methanol followed by addition of NaOMe (1 mmol, 54.0 mg) with continuous stirring. Immediate formation of dark green precipitate indicated the progress of the reaction. After 30 min stirring at room temperature, the reaction mixture was sealed in a Teflon-lined stainless steel vessel (23 mL) and heated at 150 °C for 24 h under autogenous pressure. Slow cooling to room temperature yielded dark green crystals of complex **2**. Isolated yield: 32% (based on copper). Anal. Calcd. for **3**, $C_{20}H_{20}N_{18}O_{11}Cu_4$: C, 25.48; N, 26.75; H, 2.14. Found: C, 25.69; N, 26.39; H, 2.22. IR (KBr, cm^{-1}): 3410, *ν*(NH); 3312, *ν*(OH); 1643, *ν*(C═N); 1572, 1462, 1384, 1326 and 1031.

Synthesis of $[Cu_2Ni_2(pmad)_2(pmadH)_2Cl_2](H_2O)$ (3)

$Cu(NO_3)_2{\cdot}3H_2O$ (0.25 mmol, 60.5 mg), $NiCl_2{\cdot}6H_2O$ (0.25 mmol, 60.0 mg) and 2-pyrimidineamidoxime (0.5 mmol, 69.0 mg) were dissolved in a 15 mL mixture of distilled water and methanol (2 : 1). Solid NaOMe (1 mmol, 54.0 mg) was added to the above mixture in portions. The resulting mixture was sealed in a Teflon-lined stainless steel vessel (23 mL) and heated at 150 °C for 24 h under autogenous pressure. Slow cooling to room temperature yielded dark brown crystals of complex **3**. Isolated yield: 39% (based on copper). Anal. Calcd. for **3**, $C_{20}H_{20}N_{16}O_5Cl_2Cu_2Ni_2$: C, 27.30; N, 25.47; H, 2.29. Found: C, 27.59; N, 25.29; H, 2.33. IR (KBr, cm^{-1}): 3410, *ν*(NH); 3269, *ν*(OH); 1644, *ν*(C═N); 1568, 1467, 1389, 1279 and 1090.

X-ray crystallographic data collection and refinements

Single crystal X-ray data of **1**, **2** and **3** were collected on a Bruker SMART APEX CCD diffractometer using SMART/SAINT software.[23] Intensity data were collected using graphite-monochromatized Mo-Kα radiation (0.71073 Å) at 293 K. The structures were solved by direct methods using the SHELX-97[24] program incorporated into WinGX.[25] Empirical absorption corrections were applied with SADABS.[26] All non-hydrogen atoms were refined with anisotropic displacement co-efficients. The hydrogen atoms bonded to carbon were included in geometric positions and given thermal parameters equivalent to 1.2 times those of the atom to which they were attached. The hydrogen atoms attached to the oxygen atoms of non-coordinating water molecules for the complexes **2** and **3** were located from differential Fourier maps. Structures were drawn using either ORTEP-3[27] or PLUTON.[28] The crystallographic refinement parameters are presented in Table 1 and selected bond distances and angles are listed in Table 2.

Computational details

Theoretical calculations have been carried out using the following computational methodology.[29] Using a phenomenological Heisenberg Hamiltonian $H = -\Sigma J_i S_j S_k$ (where i labels the different kinds of coupling constants, while j and k refer to the different paramagnetic centers) to describe the exchange coupling between each pair of transition-metal ions present in the polynuclear complexes, the full Hamiltonian matrix for the entire system was constructed. Exchange coupling parameters (J) were obtained by taking into account the energy difference between high-spin state and broken symmetry low-spin state. The hybrid B3LYP functional[30] has been used in all calculations as implemented in the *Gaussian 03* package.[31–32] The use of non-projected energy of the broken-symmetry solution as the energy of the low spin state within the DFT framework provides more or less satisfactory results avoiding the cancellation of the non-dynamic correlation effects.[33] LANL2DZ basis set was considered for all the elements.

Results and discussion

Syntheses of the complexes

The 1 : 1 reaction of the protonated ligand 2-pyrimidineamidoxime ($pmadH_2$) with copper(II) nitrate in methanol at room temperature yielded a 1D-copper(II) coordination polymer $[Cu(pmadH_2)_2(NO_3)](NO_3)$ (**1**). The $pmadH_2$ acts as a neutral ligand where the two ionisable groups (–NH_2 and –OH) remain protonated. A similar reaction in aqueous methanol in the presence of NaOMe under autogenous pressure at 150 °C for 24 h afforded the isolation of tetranuclear collapsed metallacrown $[Cu_4(pmad)_2(pmadH)_2(NO_3)](NO_3)(H_2O)$ (**2**). The metallacrown **2** was also prepared successfully in the absence of NaOMe under hydrothermal conditions. Both the dianionic and monoanionic forms of $pmadH_2$ are present in **2**. Similarly, reaction of equimolar amounts of copper(II) nitrate and nickel(II) chloride with two equivalents of $pmadH_2$ led to the formation of the heteronuclear complex $[Cu_2Ni_2(pmad)_2(pmadH)_2Cl_2](H_2O)$ (**3**) under similar reaction conditions. A synthetic strategy for the preparation of complexes **1–3** is summarized in Scheme 2. All the complexes are essentially insoluble in common organic solvents, except **1** which is soluble in water. The presence of both Cu^{II} and Ni^{II} in complex **3** was confirmed by X-ray photoelectron spectroscopy (ESI, Fig. S1, S2†).[34] The bands due to both Cu^{II} and Ni^{II} were observed in the XPS spectrum for **3**.

Table 1 Crystallographic data and refinement parameters for complexes **1–3**

	1	**2**	**3**
Empirical formula	$C_{10}H_{12}N_{10}O_8Cu$	$C_{20}H_{20}N_{18}O_{11}Cu_4$	$C_{20}H_{18}N_{16}O_6Cl_2Cu_2Ni_2$
Fw	463.85	942.74	893.85
T/K	293 (2)	293 (2)	293 (2)
Crystal system	Triclinic	Monoclinic	Triclinic
Space group	$P\bar{1}$	$C2/c$	$P\bar{1}$
a/Å	7.0434(2)	27.924(6)	8.6134(11)
b/Å	8.7481(3)	16.597(3)	9.7382(12)
c/Å	13.6485(4)	15.514(3)	10.3083(13)
α (°)	98.392(2)	90.00	66.030(2)
β (°)	92.024(2)	121.934(8)	83.795(2)
γ (°)	97.262(1)	90.00	65.826(2)
V/Å^3	824.05(4)	6101.88(2)	719.03(2)
Z	2	8	1
ρ_c/g cm^{-3}	1.8692	2.050	2.074
μ(Mo-Kα)/mm^{-1}	1.398	2.841	3.005
λ/Å	0.71073	0.71073	0.71073
F(000)	470.0	3752.0	450.0
collected reflns	12999	45532	7421
unique reflns	5008	5375	2921
$R_{(int)}$	0.0268	0.0887	0.0251
GOF (F^2)	1.040	1.240	1.087
R_1[a]	0.0405	0.0659	0.0316
wR_2[b]	0.1081	0.2403	0.0817

[a] $R_1 = \Sigma \| F_o | - | F_c \| / \Sigma | F_o |$, [b] $wR_2 = [\Sigma \{ w(F_o^2 - F_c^2)^2 \} / \Sigma \{ w(F_o^2)^2 \}]^{1/2}$.

Table 2 Selected bond distances (Å) and angles (°) for **1**, **2** and **3**

1					
Cu(1)–N(1)	2.034(2)	Cu(1)–N(2)	1.972(2)	Cu(1)–N(3)	2.029(2)
Cu(1)–N(4)	1.975(2)	Cu(1)–O(3)	2.308(2)	Cu(1)–O(5)	2.770(2)
O(1)–N(2)	1.408(2)	O(2)–N(4)	1.403(3)	O(3)–N(9)	1.270(3)
O(4)–N(9)	1.258(3)	O(5)–N(9)	1.218(3)	O(6)–N(10)	1.243(3)
O(7)–N(10)	1.230(3)	O(8)–N(10)	1.213(3)	N(2)–C(5)	1.296(3)
N(4)–C(10)	1.294(3)	N(3)–C(6)	1.339(3)	N(8)–C(10)	1.328(3)
N(2)–Cu(1)–N(4)		177.12(8)		N(2)–Cu(1)–N(3)	100.07(7)
N(4)–Cu(1)–N(3)		80.51(7)		N(2)–Cu(1)–N(1)	79.88(7)
N(4)–Cu(1)–N(1)		100.87(8)		N(3)–Cu(1)–N(1)	153.75(7)
N(2)–Cu(1)–O(3)		88.89(7)		N(4)–Cu(1)–O(3)	88.26(7)
N(3)–Cu(1)–O(3)		109.62(7)		N(1)–Cu(1)–O(3)	96.63(6)
2					
Cu(1)–N(4)	1.941(5)	Cu(1)–N(3)	2.026(5)	Cu(1)–O(2)	1.924(5)
Cu(1)–O(3)	1.945(5)	Cu(2)–N(5)	1.881(6)	Cu(2)–N(9)	2.014(5)
Cu(2)–N(6)	1.926(5)	Cu(2)–O(2)	1.920(4)	Cu(3)–N(2)	1.895(6)
Cu(3)–N(16)	1.916(5)	Cu(3)–O(1)	1.911(4)	Cu(3)–N(10)	1.989(5)
Cu(4)–O(1)	1.931(5)	Cu(4)–O(4)	1.947(4)	Cu(4)–N(1)	1.960(5)
Cu(4)–N(11)	2.002(5)	Cu(4)–O(5)	2.400(6)	O(1)–N(4)	1.415(6)
O(2)–N(1)	1.407(6)	O(3)–N(6)	1.361(7)	O(4)–N(16)	1.351(7)
N(4)–C(1)	1.320 (8)	N(1)–C(5)	1.310(8)	N(16)–C(3)	1.290(8)
N(6)–C(4)	1.308 (8)				
O(2)–Cu(1)–N(4)		100.8(2)		O(2)–Cu(1)–O(3)	89.7(2)
N(4)–Cu(1)–N(3)		80.9(2)		N(4)–Cu(1)–O(3)	169.5(2)
O(2)–Cu(1)–N(3)		177.0(2)		O(3)–Cu(1)–N(3)	88.8(2)
N(5)–Cu(2)–O(2)		83.6(2)		N(5)–Cu(2)–N(6)	170.5(2)
O(2)–Cu(2)–N(6)		86.9(2)		N(5)–Cu(2)–N(9)	107.4(2)
O(2)–Cu(2)–N(9)		168.7(2)		N(6)–Cu(2)–N(9)	82.1(2)
N(2)–Cu(3)–O(1)		83.7(2)		N(2)–Cu(3)–N(16)	170.0(2)
O(1)–Cu(3)–N(16)		87.7(2)		N(2)–Cu(3)–N(10)	107.3(2)
O(1)–Cu(3)–N(10)		168.4(2)		N(16)–Cu(3)–N(10)	81.6(2)
O(1)–Cu(4)–O(4)		90.4 (2)		O(1)–Cu(4)–N(1)	99.4(2)
O(4)–Cu(4)–N(1)		167.2(2)		O(1)–Cu(4)–N(11)	170.4(2)
O(4)–Cu(4)–N(11)		87.7(2)		N(1)–Cu(4)–N(11)	81.2(2)
O(1)–Cu(4)–O(5)		88.1(2)		O(4)–Cu(4)–O(5)	97.1(2)
N(1)–Cu(4)–O(5)		91.4(2)		N(11)–Cu(4)–O(5)	101.5(2)
3					
Cu(1)–N(5)	2.028(3)	Cu(1)–N(7)	1.992(3)	Cu(1)–O(1)$^{\#1}$	1.990(2)
Cu(1)–O(2)$^{\#1}$	1.965(2)	Cu(1)–Cl(1)	2.474(1)	Ni(1)–N(1)	1.934(3)
Ni (1)–N(3)	1.892(3)	Ni (1)–N(8)	1.857(3)	Ni (1)–O(2)	1.875(2)
C(5)–N(4)	1.336(4)	C(10)–N(8)	1.329(4)	N(3)–O(1)	1.355(3)
N(7)–O(2)	1.404(3)				
N(5)–Cu(1)–N(7)		79.69(10)		N(7)–Cu(1)–O(2)$^{\#1}$	97.85(9)
O(2)$^{\#1}$–Cu(1)–O(1)$^{\#1}$		87.79(9)		O(1)$^{\#1}$–Cu(1)–N(5)	88.01(10)
Cl(1)–Cu(1)–O(1)$^{\#1}$		97.32(8)		Cl (1)–Cu(1)–O(2)$^{\#1}$	101.28(8)
Cl (1)–Cu(1)–N(5)		97.80(8)		Cl (2)–Cu(1)–N(7)	102.37(9)
N(7)–Cu(1)–O(1)$^{\#1}$		157.98(11)		N(5)–Cu(1)–O(2)$^{\#1}$	160.84(11)
N(1)–Ni(1)–N(3)		82.52(11)		N(1)–Ni(1)–N(8)	103.59(12)
N(8)–Ni(1)–O(2)		84.45(10)		N(3)–Ni(3)–O(2)	89.42(10)
N(8)–Ni(3)–N(3)		173.84(11)		N(1)–Ni(3)–O(2)	171.68(11)

Symmetry transformations used to generate equivalent atoms: #1 −x+2, −y, −z+1.

Structure description of [Cu(pmadH$_2$)$_2$(NO$_3$)](NO$_3$) (1)

The asymmetric unit of complex **1** contains one crystallographically unique Cu^{II} ion, two pmadH$_2$ ligands and two different nitrate ions. One of the nitrate ions bridges the Cu^{II} ions to form a 1D chain (along crystallographic *a* axis) structure whereas the other nitrate ion acts as a counter anion. Two pmadH$_2$ ligands act as bidentate neutral blocking NN donors occupying the equatorial plane to form a stable five member chelate ring. The axial positions are occupied by the oxygen atoms from bridging nitrates (Fig. 1). The coordination environment around the central Cu^{II} atom is distorted octahedral with four relatively short equatorial bonds and two considerably longer axial bonds. While the equatorial Cu–N bonds range narrowly between 1.972(2) and 2.034(2) Å (Table 2), the axial bonds vary by almost 0.5 Å [Cu(1)–O(3), 2.308(2) Å; Cu(1)–O(5), 2.770(2) Å]. The solid state packing diagram for complex **1** shows that the 1D chains run parallel (Fig. 2 top) to each other with an interchain Cu(1)···Cu(1) distance of 8.748(5) Å along the crystallographic *b* axis. Interestingly, the adjacent intermolecular aromatic rings lean towards each other due to π-stacking interaction (distance between the centroids of the six planar atoms N6, C5, C4, N5, C3 and C2 of the adjacent chains is 3.35 Å, Fig. 2). Presumably due to such π-stacking interaction, the equatorial coordination around Cu^{II} is distorted from the planar geometry with an r.m.s deviation of 0.24 Å.

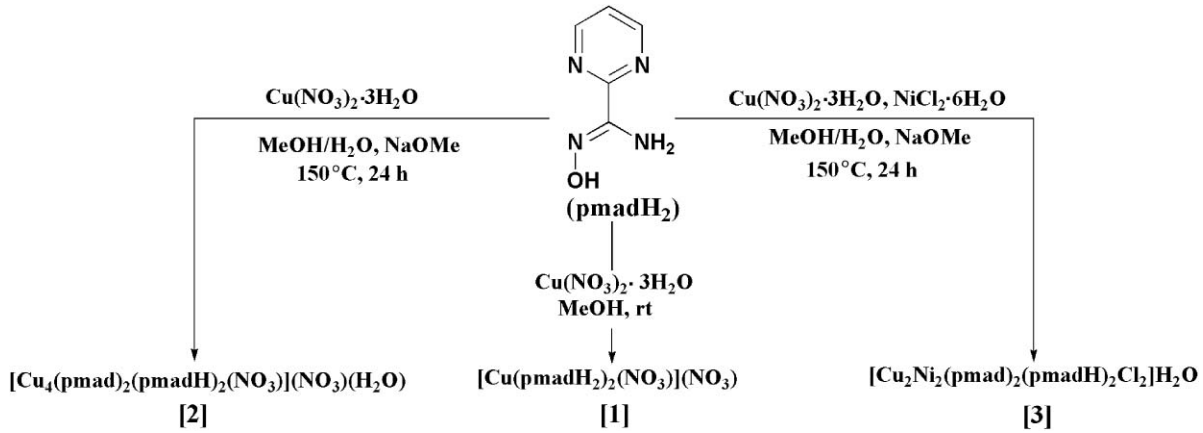

Scheme 2 The schematic representation of the synthesis of complexes **1–3**.

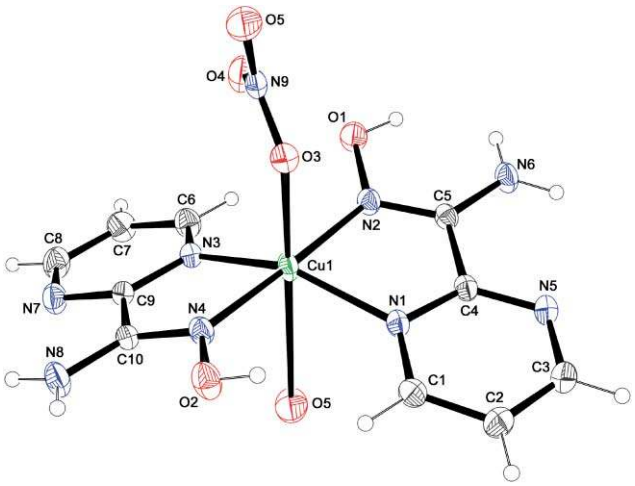

Fig. 1 ORTEP (30% probability) view of the basic unit of **1**.

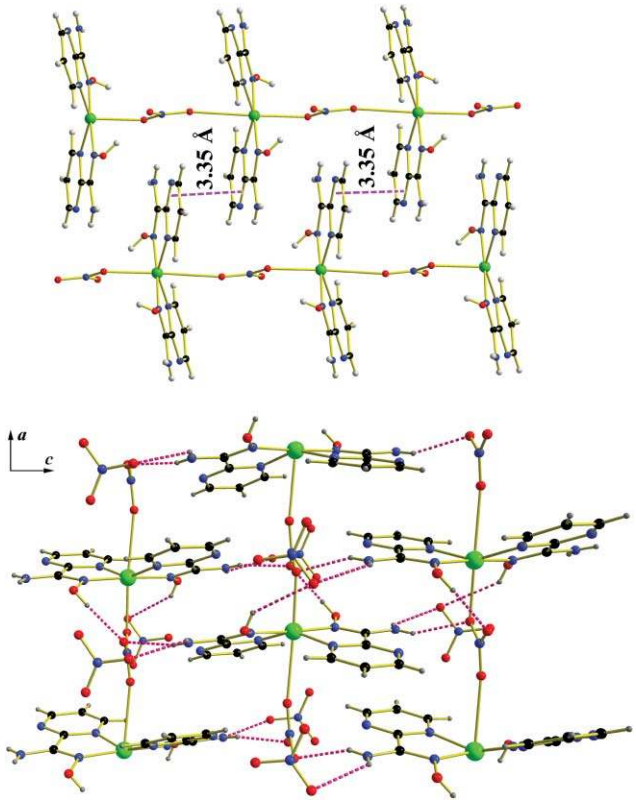

Fig. 2 Packing diagram of complex **1** forming a one-dimensional chain along the crystallographic *a* axis (top). View of the 2D H-bonded network of **1** (bottom). Dotted lines represent H-bonding. Color codes: Green = Cu^{II}, blue = N, red = O, black = C, gray = H.

In the crystal structure, one of the *trans* N–Cu–N angles is near to 180° [N(2)–Cu(1)–N(4), 177.12(8)°], the other one [N(3)–Cu(1)–N(1), 153.75(7)°] significantly deviates from linearity and consequently the *trans* coordinated oxygen atom is tilted away from the normal of the equatorial plane with an O(3)–Cu(1)–O(5) angle of 169.27(7)°. The distance between two nearest Cu^{II} centers is found to be 7.043(4) Å. Several intramolecular and intermolecular H-bonding interactions were observed in the packing diagram of complex **1**. Two adjacent chains are connected to each other through H-bonds, with $O2\cdots O7^{\#1} = 2.728(4)$ Å (#1: x–1, y, z) and $\angle O2–H9\cdots O7^{\#1} = 160(4)°$ (ESI, Table S1†). The oxygen atoms of the coordinated and non-coordinated nitrates also participate in H-bonding with the free $–NH_2$ and –OH groups of the ligand to form a two-dimensional network (Fig. 2).

Structure description of $[Cu_4(pmad)_2(pmadH)_2(NO_3)](NO_3)(H_2O)$ (2)

Complex **2** crystallizes in monoclinic *C*2/*c* space group with an asymmetric unit containing four unique Cu^{II} ions, two monoanionic pmadH, two dianionic pmad, two different nitrate anions and a non-coordinated water molecule (Fig. 3). The axial site of one of the four Cu^{II} [Cu(4)] is coordinated to a nitrate ion forming penta-coordinated square pyramidal geometry whereas the other three Cu^{II} [Cu(1,2,3)] centers are in a square planar geometry. The diagonally opposite Cu^{II} ions [Cu(2) and Cu(3)] have almost similar equatorial bonding environments with each of the copper atoms being bonded to three nitrogen atoms and an oxygen atom. The Cu–N distances for Cu(2) and Cu(3) range from 1.881(6)–2.014(5) Å and 1.895(6)–1.989(5) Å, respectively. The Cu–O distances for Cu(2) and Cu(3) are 1.920(4) and 1.911(4) Å, respectively. On the other hand Cu(1) and Cu(4) are equatorially bonded to two nitrogen atoms [Cu(1)–N, 1.941(5)–2.026(5) Å; Cu(4)–N, 1.960(5)–2.002(5) Å] and two oxygen atoms [Cu(1)–O,

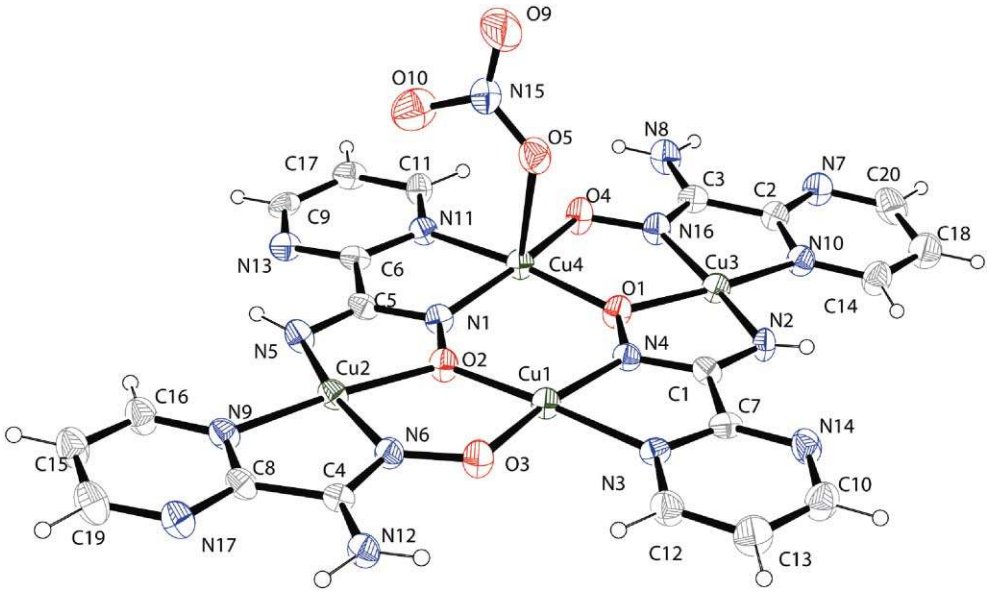

Fig. 3 ORTEP view (30% probability) of the molecular structure of **2**.

1.924(5)–1.945(5) Å; Cu(4)–O, 1.931(5)–1.947(4) Å] *trans* to each other. Additionally, Cu(4) is also bonded apically to an oxygen atom [Cu(4)–O(5), 2.400(6) Å] of a nitrate anion. Interestingly, the Cu(4) is slightly pushed up towards the axial nitrate with a distance of 0.06 Å from the equatorial plane. The torsion angles between Cu(1)···Cu(2) and Cu(3)···Cu(4) through –N–O– bridges are deviated from the planarity by only ~1°. Out of the four oxo groups in the skeleton, two doubly bridging oxo groups are oriented towards the center of the complex whereas the other two are pointed towards the periphery of the complex. Cu(1) and Cu(4) are separated by 3.882(5) Å and generate the central planar Cu^{II}-$(N–O)_2$-Cu^{II} hexagonal core. But the other two Cu^{II} atoms [Cu(2) and Cu(3)] are far from each other [7.179(11) Å]. The distances between Cu(1)···Cu(2) [3.352(5) Å] and Cu(3)···Cu(4) [3.328(5) Å] are almost the same. The structure of this complex is best described as a collapsed 12-MC-4 with four metal centers and four bridging –N–O– moieties forming an almost planar crown structure. The two ring-oxygens of the metallacrown bind to ring Cu^{II} centers on the opposite side of the MC ring producing a collapsed 12-MC-4 (Fig. 4). Since the core is collapsed, the six-membered ring generated at the center does not allow encapsulation of cations or anions.

As depicted in Fig. 5, each molecule interacts with the four neighboring molecules through H-bonds to form a two-dimensional layer. The coordinated and noncoordinated nitrates in the tetranuclear unit act as acceptors. The lattice water molecule, however, acts both as acceptor and donor to form H-bonding with the donor $–NH_2$ and –NH groups of the other molecules. The N2 acts as a donor to form H-bonding with O1W of the water molecule with N2···O1W distance 3.186(10) Å, and ∠N2–H2···O1W = 149(6)° (ESI, Table S2†). The N5 acts as a donor and forms a H-bond to the noncoordinated nitrate with a N5···$O7^{\#1}$ distance of 3.317(11) Å (#1: x–1/2, y–1/2, z–1) and ∠N5–H5···$O7^{\#1}$ = 134(5)°. The O1W water molecule acts as a donor to form a H-bond to both $O9^{\#5}$ (#5: x+1/2, –y+1/2, z+1/2) and O7 of coordinated and noncoordinated nitrate respectively, with

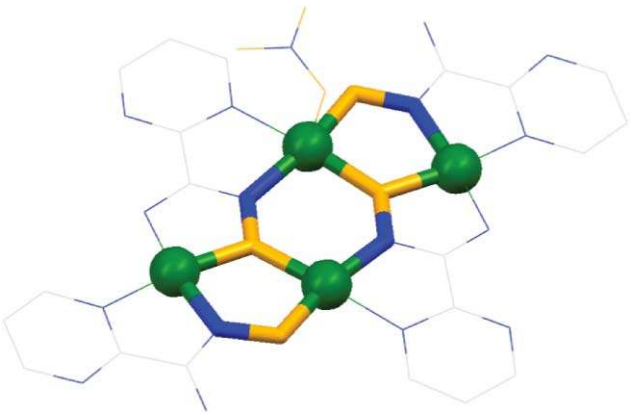

Fig. 4 The structure of the collapsed 12-$MC_{Cu(II)}$-4 complex **2** with the MC ring highlighted. Two ring oxygens bind across the core to two ring Cu^{II} ions, which cause the cavity to collapse. Color scheme: green sphere = Cu^{II}; orange tube = O; blue tube = N; gray line = C. Hydrogen atoms have been omitted for clarity.

O1W···$O9^{\#5}$ distance of 2.990(11) Å and ∠O1W–H1W···$O9^{\#5}$ = 158(9)°; O1W···O7 = 3.029(12) Å and ∠O1W–H2W···O7 = 179(8)°. Consequently, the tetranuclear unit is associated with its neighbors through double hydrogen bonds [with N12···$O5^{\#4}$ (#4: –x, –y, –z+1) distance of 2.971(8) Å] and results in two Cu^{II} ions coming closer to each other with Cu1···Cu1 [–x, –y, –z+1] = 3.591(4) Å.

Structure description of $[Cu_2Ni_2(pmad)_2(pmadH)_2Cl_2](H_2O)$ (3)

Complex **3** crystallizes in the triclinic $P\bar{1}$ space group with one unique Cu^{II}, one unique Ni^{II}, one monoanionic pmadH, one dianionic pmad, one bonded chloride and a noncoordinated water molecule in its asymmetric unit. The Ni^{II} ions have a square planar coordination environment, while the Cu^{II} ions have distorted square pyramidal geometry (Fig. 6). The Cu^{II} atoms are pulled towards axial chlorine and lie 0.18 Å above the equatorial

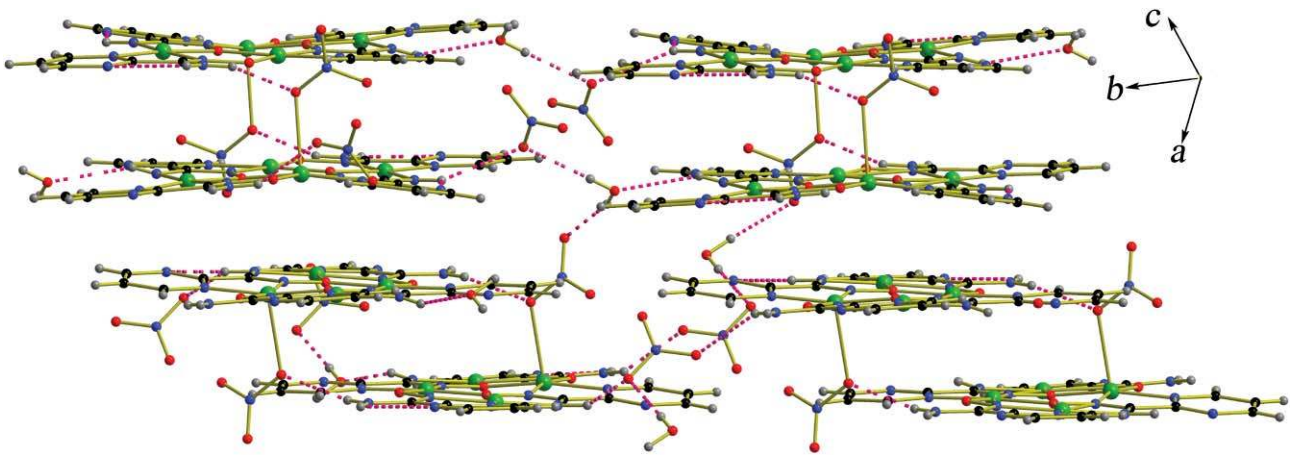

Fig. 5 View of the two-dimensional H-bonded network of **2**. Color codes: green = Cu(II); red = oxygen; blue = nitrogen; gray = carbon; gray = hydrogen.

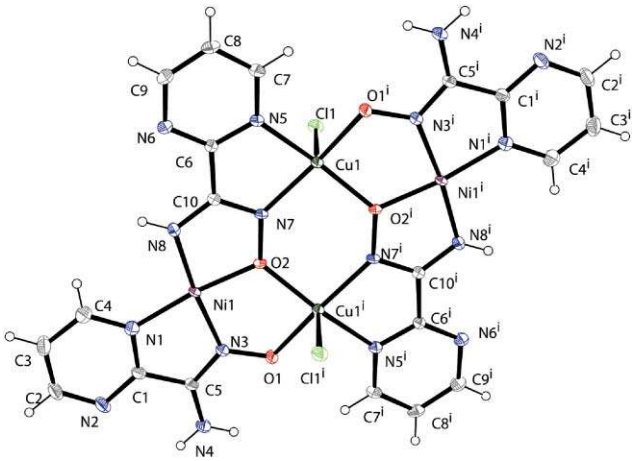

Fig. 6 ORTEP view (30% probability) of the molecular structure of **3**.

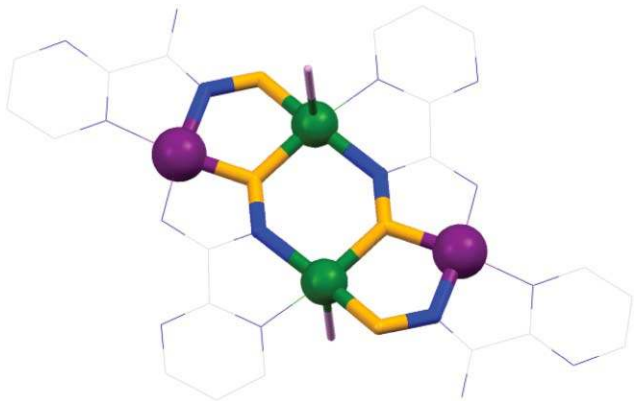

Fig. 7 The structure of the collapsed 12-$MC_{Cu(II)Ni(II)}$-4 complex **3** with the MC ring highlighted. Two ring-oxygens bind across the core to two ring Cu^{II} ions giving a collapsed structure. Color schemes: green sphere = Cu^{II}; violet sphere = Ni^{II}; orange tube, oxygen; blue tube, nitrogen; pink tube, chlorine; gray line, carbon. Hydrogen atoms have been removed for clarity.

plane. The axial bond length of 2.474(2) Å [Cu(1)–Cl(1)] is relatively longer than the average equatorial bond lengths (1.99 Å). Each Cu^{II} atom is bonded to two nitrogen atoms [Cu(1)–N(5), 2.028(3) Å; Cu(1)–N(7), 1.992(3) Å] and two oxygen atoms [Cu(1)–O(1), 1.990(2) Å; Cu(1)–O(2), 1.965(2) Å] in the equatorial plane, whereas the Ni^{II} atoms are bonded to three nitrogen atoms [N(1), N(3) and N(8)] with Ni–N bond distances ranging from 1.857(3) to 1.933(3) Å and an oxygen atom [Ni(1)–O(2), 1.875(2) Å] (*trans* to the aromatic N). The Ni^{II} ions preferentially occupy square planar geometry with three nitrogen coordination. While the equatorial sites around square pyramidal Cu^{II} are satisfied by two oxygens and two nitrogens. Such an observation is consistent with previous reports where, in general, nickel ions with a five membered chelate ring preferred square planar geometry.[19e]

The metallacrown structure of complex **3** is very similar to that of **2** and it also has a cavity collapsed 12-MC-4 structure with a central hexagonal ring (Fig. 7). The central hexagonal ring contains two Cu^{II} centers with a Cu···Cu distance of 3.966(7) Å and two –N–O– linkages. The distance between two Ni^{II} centers is 7.105(9) Å and that of between the nearest Cu^{II} and Ni^{II} [–x+2, –y, –z+1] is 3.285(6) Å.

As shown in Fig. 8, complex **3** interacts with six neighboring molecules through intermolecular H-bonding to form a three-dimensional network. The chlorine atoms act as acceptors while the $–NH_2$ groups of neighboring molecules act as donors with a N4···Cl1$^{\#1}$ distance of 3.455(3) Å and ∠N4–H4A···Cl1$^{\#1}$ = 145(4)°. H-bonding interaction is also observed between the nitrogen atom in the aromatic ring and the free $–NH_2$ group of the other molecule in the same plane. This is running in the crystallographic *b* direction with N4···N2$^{\#2}$ distance of 3.341(4) Å (#2: –x+1, –y+2, –y) and ∠N4–H4B···N2$^{\#2}$ = 146(4)°. The –NH groups of **3** acts as donors to a water molecule and extend towards the crystallographic *a* axis with N8···O1W$^{\#3}$distance of 3.100(5) Å and ∠N8–H8···O1W$^{\#3}$ = 166(3)°. H-bond parameters for complex **3** are given in Table S3 (ESI†).

Magnetic behavior

Complex 2. The plots of both χ_M *vs.* T and $\chi_M T$ *vs.* T for **2** per Cu^{II}_4 unit are shown in Fig. 9. Room temperature (300 K) $\chi_M T$ value of 1.58 cm^3 K mol^{-1} is slightly higher than the expected value for four uncoupled Cu^{II} ions ($\chi_M T$ = 0.375 cm^3 K mol^{-1} for a S = 1/2 ion). As the temperature is lowered, $\chi_M T$ value remains virtually constant up to about 25 K, below which it increases slightly and reaches a maximum at 16 K (1.70 cm^3 K mol^{-1}). Below

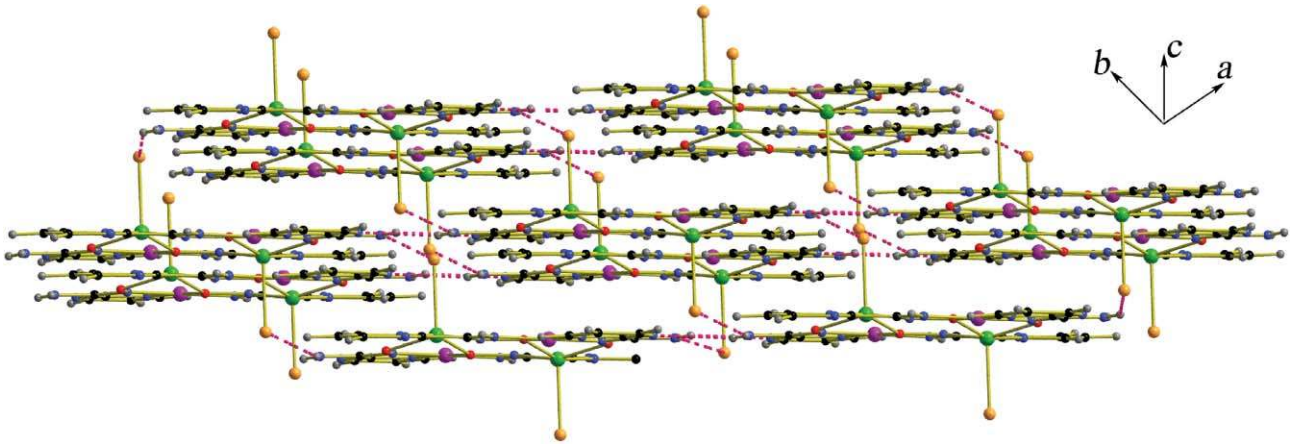

Fig. 8 View of the 3D hydrogen bonded network of **3**. Color codes: green = Cu^{II}; purple = Ni^{II}; orange = chlorine; red = oxygen; blue = nitrogen; black = carbon; and gray = hydrogen.

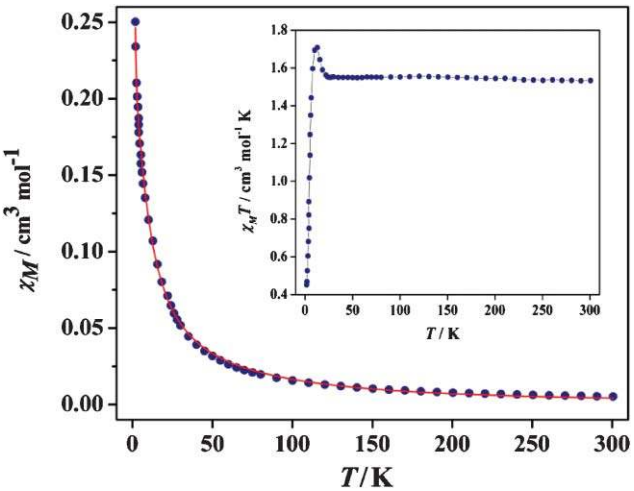

Fig. 9 The plots of χ_M *vs.* T and $\chi_M T$ *vs.* T (inset) for **2**. The red line corresponds to the best fit.

this temperature the $\chi_M T$ value falls rapidly to 0.45 cm^3 K mol^{-1} at 1.8 K probably due to the low temperature antiferromagnetic interaction. The $1/\chi_M$ *vs.* T plot (300–1.8 K) obeys the Curie–Weiss law with a positive Weiss constant of θ = 5.0 K (ESI, Fig. S4†). The nature of the $\chi_M T$ *vs.* T plot and the low positive value of θ suggest the presence of both ferromagnetic and antiferromagnetic exchange interactions among the four Cu^{II} ions through –N–O– and –O– bridges.

Though the four Cu^{II} centers are not crystallographically equivalent, the similarities in the bridging modes and the coordination environment within the crown framework gives rise to two sets of roughly magnetically equivalent Cu^{II} atoms and thus only two kinds of magnetic exchange pathways (J_1 and J_2; Scheme 3) were considered for the analysis of experimental data.

A reasonable fit was obtained for non-interacting tetranuclear units applying the conventional Hamiltonian:

$$H = -J_1(S_1 \cdot S_2 + S_3 \cdot S_4) - J_2(S_1 \cdot S_4 + S_2 \cdot S_3) \quad (1)$$

The theoretical expression for the magnetic susceptibility per Cu_4 unit obtained from the above Hamiltonian is given in eqn (2).

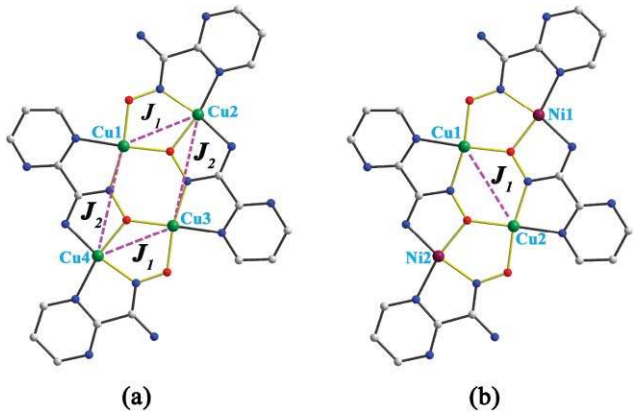

Scheme 3 The magnetic pathways in complexes **2** and **3** between paramagnetic centers.

$$\chi_M = (Ng^2\beta^2/KT)[A/B] \quad (2)$$

Where, $A = [30\exp(-E_1/kT) + 6\exp(-E_2/kT) + 6\exp(-E_3/kT) + 6\exp(-E_4/kT)]$ and $B = 5[\exp(-E_1/kT) + 3\exp(-E_2/kT) + 3\exp(-E_3/kT) + 3\exp(-E_4/kT) + \exp(-E_5/kT) + \exp(-E_6/kT)]$.

The parameters N, β and k have their usual meanings and E_n values were obtained using the Kambe method[35] from the Hamiltonian.

$E_1 = (-J_1 - J_2)/2$, $E_2 = (-J_1 + J_2)/2$, $E_3 = (J_1 + J_2)/2$, $E_4 = (J_1 - J_2)/2$, $E_5 = (J_1 + J_2)/2 + (J_1^2 + J_2^2 - J_1J_2)^{1/2}$, $E_6 = (J_1 + J_2)/2 - (J_1^2 + J_2^2 - J_1J_2)^{1/2}$.

The best fit parameters obtained are J_1 = +10.7 cm^{-1}, J_2 = −2.7 cm^{-1} and g = 2.1 with $R = 5.6 \times 10^{-5}$, where $R = \sum[(\chi_M T)_{exp} - (\chi_M T)_{cal}]^2/\sum(\chi_M T)_{exp}^2$.

Complex 3. Fig. 10 shows the temperature dependence of χ_M and $\chi_M T$ values for complex **3**. The room temperature $\chi_M T$ = 0.77 cm^3 K mol^{-1} is very close to the expected value for two uncoupled Cu^{II} ions. The room temperature magnetic susceptibility value indicates the diamagnetic nature of Ni^{II}, lending support to the coordination environment around nickel atoms in complex **3** being square planar rather than square pyramidal in which case the magnetic susceptibility value would have been much higher. The $\chi_M T$ value gradually decreases upon cooling and reaches a

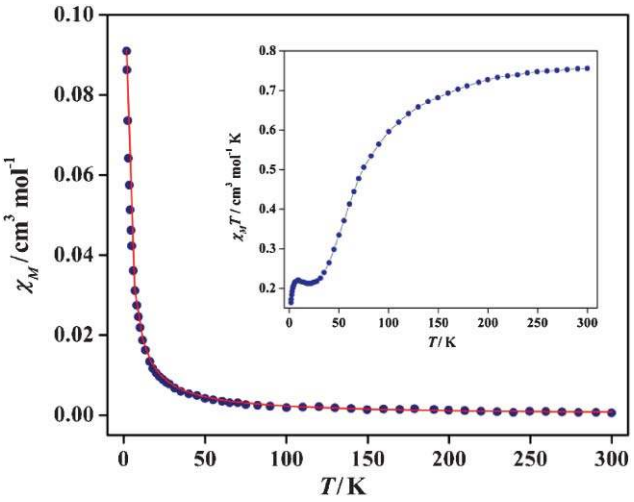

Fig. 10 Plots of χ_M *vs.* T and $\chi_M T$ *vs.* T (inset) for **3**. The red line corresponds to the best fit.

minimum (0.21 cm^3 mol^{-1} K) at 26 K. Further cooling increases the $\chi_M T$ value very slightly up to about 10 K (0.22 cm^3 mol^{-1} K) before further falling to 0.16 cm^3 mol^{-1} K at 1.8 K. The $1/\chi_M$ *vs.* T plot (300–1.8 K) obeys the Curie–Weiss law with a negative Weiss constant $\theta = -1.5$ K (ESI, Fig. S5†). The nature of the $\chi_M T$ *versus* T plot and the negative θ suggest a dominant antiferromagnetic exchange between the Cu^{II} ions through the bridging pathways.

The low temperature hump at around 10 K may indicate the presence of very weak intermolecular ferromagnetic interaction. The magnetic interaction through the –N–O– bridges between two Cu^{II} atoms leads to a $S = 0$ ground state. The susceptibility data were analyzed using the Bleaney–Bowers equation.[21] The best-fit parameters obtained were $g = 2.08$ and $J_1 = -3.4$ cm^{-1} with agreement factor $R = 2.8 \times 10^{-5}$, where $R = \sum[(\chi_M T)_{exp} - (\chi_M T)_{cal}]^2 / \sum(\chi_M T)_{exp}^2$.

Thus, it was observed that in complex **2** both ferromagnetic and antiferromagnetic interactions are present. The ferromagnetic exchange coupling interaction occurs through (J_1) the –N–O– and μ_2-O bridges and antiferromagnetic coupling (J_2) takes place through only the –N–O– bridging mode giving overall weak ferromagnetic interaction. When the interaction between Cu(1) and Cu(3) in complex **2** (as in complex **3**) was included as the third exchange parameter, the fitting was not satisfactory. So we considered only two different exchange parameters and that enabled us to reproduce the experimental curve agreeably. But the negative exchange coupling constant ($J_1 = -3.4$ cm^{-1}) obtained in complex **3** shows the presence of very weak antiferromagnetic interaction between two Cu^{II} through –N–O– bridges within the hexagonal core. If we consider that this interaction exists in complex **2** as well, then also a resultant weak ferromagnetic interaction is expected. To understand the origin of the ferromagnetic and antiferromagnetic interactions we have carried out DFT calculations for complexes **2** and **3**.

EPR spectra

The X-band EPR spectra of powdered samples of **2** and **3** at different temperatures are shown in Fig. 11. The g value (2.09) for **2** remains unchanged up to 20 K (field 3214 G for $\nu = 9.4343$ GHz) and decreases to 2.08 and 2.05 at 30 K and 50 K, respectively. The intensity of the EPR spectrum increases as the temperature is lowered. The g value of 2.11 (field 3190 G for $\nu = 9.434$ GHz) for **3** is a little high at 10 K but decreases to 2.09 at 50 K. At high temperature, the EPR spectra for both the complexes are isotropic. But at low temperature (5 K and 10 K for **2**; 10 K and 20 K for **3**), the spectra are anisotropic in both cases. The anisotropy of **2** at low temperature could be due to zero-field splitting of the ground state. This implies that the susceptibility results are in accordance with the EPR findings.

DFT calculations

To investigate and understand the ferromagnetic and antiferromagnetic interactions in complexes **2** and **3**, DFT calculations were performed in broken symmetry formalism. The B3LYP functional[32–33] with LANL2DZ basis were used as implemented in the *Gaussian '03* package.[31] All calculations were carried out using atomic coordinates as obtained from the X-ray crystal structures.

Complex **2** with four unpaired electrons on four Cu^{II} gives rise to three possible spin states: quintet ($S = 2$), triplet ($S = 1$) and singlet ($S = 0$). Single point calculation of the three states shows

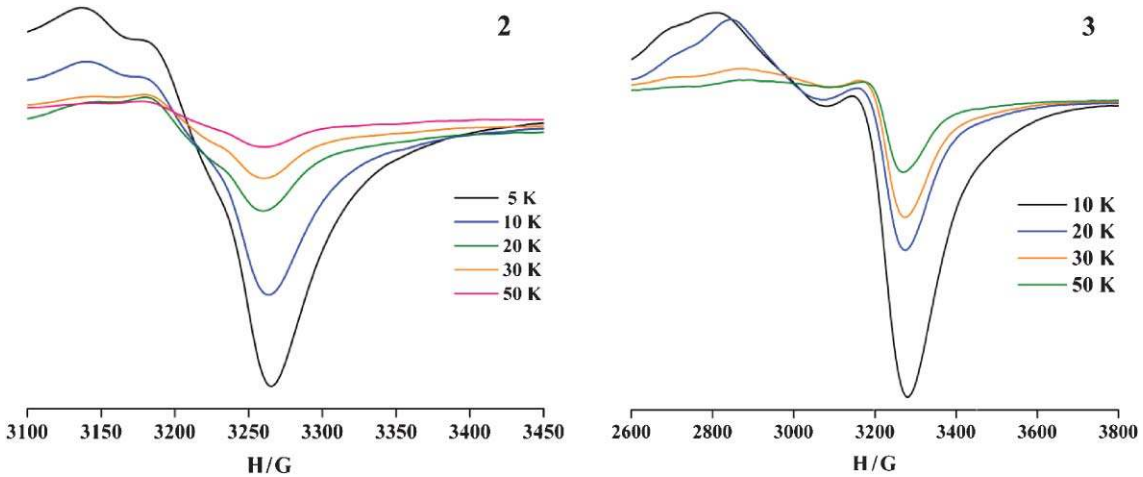

Fig. 11 The X-band EPR spectra of **2** and **3** at different temperatures.

the presence of ferromagnetic interaction in **2** with $S = 2$ (high spin state) as the ground state. The magnetic exchange parameters (J_1 and J_2) were calculated from the relative energy differences (Scheme 4) between the quintet–triplet and quintet–singlet states. The very small difference in energy (0.014 eV) between the $S = 2$ and $S = 0$ states also indicates the weak ferromagnetic behavior of **2**. The calculated magnetic exchange parameters $J_1 = +17.6$ cm^{-1} and $J_2 = -6.3$ cm^{-1} are in good agreement with the experimental results of $J_1 = +10.7$ cm^{-1} and $J_2 = -2.7$ cm^{-1}.

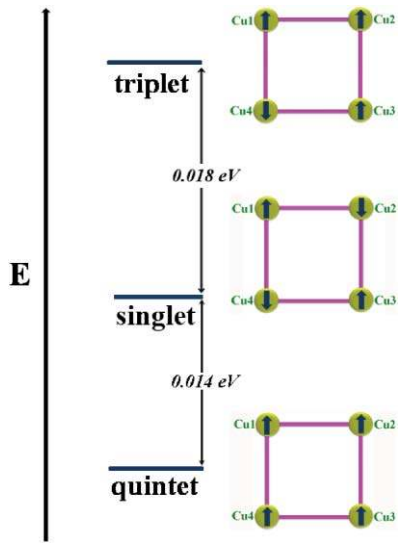

Scheme 4 The relative energies of the different spin states with the spin orientations in complex **2**.

The magnetic exchanges between Cu1 ··· Cu2 and Cu3 ··· Cu4 are mediated by the –N–O– and –O– bridges producing ferromagnetic interaction ($J_1 = +17.6$ cm^{-1}). It is well known[19,36] that the μ_2-NO bridge generally mediates antiferromagnetic interaction between paramagnetic centers. So, probably the oxo bridged pathway mediates ferromagnetic exchange in this case. It is very well established that the crossover angle (from ferromagnetic to antiferromagnetic) for the oxo bridged Cu^{II} compounds is around 98°.[29a,37] Hence the ferromagnetic interaction through the oxo bridge having a large Cu–O–Cu angle 121.41° is an unusual observation. The magnetic couplings between Cu1 ··· Cu4 and Cu2 ··· Cu3 are mediated *via* only –N–O– bridges resulting in the antiferromagnetic interactions.

The DFT calculation for complex **3** illustrates the presence of very weak antiferromagnetic interaction in the molecule. The diamagnetic nature of the two square planar Ni^{II} centers implies that there are only two possible spin states for **3** with two unpaired electrons from the two Cu^{II} centers: triplet ($S = 1$) and singlet ($S = 0$) (Scheme 5). The single point calculation shows that the broken symmetry singlet state is the most stable, which in turn implies the antiferromagnetic behavior of **3**. The calculated exchange coupling constant $J_1 = -5.7$ cm^{-1} is in good agreement with the experimental result of -3.4 cm^{-1}. The magnetic exchange between Cu^{II} centers is carried out through the two oximato –N–O– bridges which are generally expected to mediate antiferromagnetic interaction.

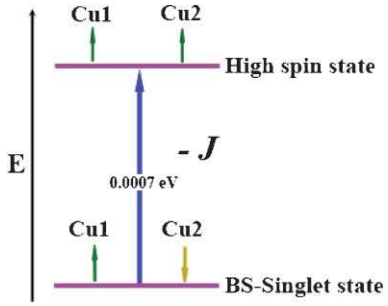

Scheme 5 The relative stability of the two possible spin states as obtained from DFT and the energy difference between these two states with spin orientations in complex **3**.

To understand the role of the bridging moieties in the weak magnetic interactions of both the complexes we analyzed the spin density distribution on the paramagnetic centers as well as on the bridging atoms. The atomic spin density of the Cu^{II} and the bridging atoms in both the complexes in all of their spin states are compiled in Tables S4 and S5 in the ESI.† The spin density maps of all the possible states of complex **2** are shown in Fig. 12. The spin densities in the high spin state (quintet) on Cu1 and Cu2 are considerably lower (average 0.34 e$^-$) compared to that on Cu3 and Cu4 on the other side (average 0.55 e$^-$). This can be attributed to the strong ferromagnetic interaction between Cu1 ··· Cu2 as compared to Cu3 ··· Cu4. The large spin densities on the oxygen atoms of the oxo bridges (average 0.19 e$^-$) indicate the strong ferromagnetic interaction through the oxo-bridge. The spin densities on the N and O atoms (average 0.11 e$^-$) of the oximato –N–O– bridges are significantly low as expected for a weak antiferromagnetic mediator.

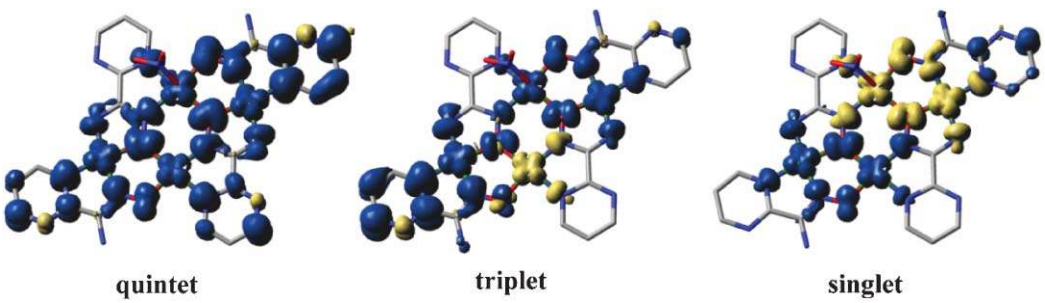

Fig. 12 The spin density maps of all the spin states of complex **2**. The blue and yellow surfaces represent the α and β spins, respectively. The isodensity surfaces correspond to a value of 0.002 e/b^3.

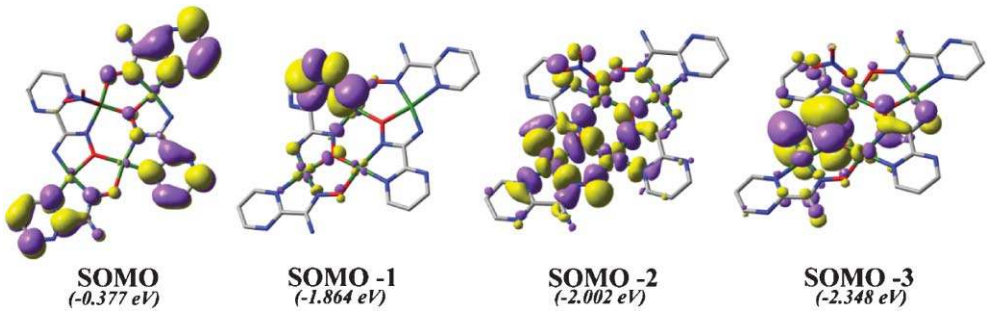

Fig. 13 The SOMOs of complex **2**. Violet and yellow surfaces represent two different symmetry orbitals. The isodensity surfaces correspond to a value of 0.001 e/b^3.

A similar calculation on complex **3** (ESI, Fig. S8†) showed that most of the spin density concentrated on the Cu^{II} centers in both the spin states. The negligibly small spin densities on the Ni^{II} centers in both states confirmed their diamagnetic nature. The spin delocalization on the nitrogen and oxygen atoms of the oximato –N–O– groups was not significant (average 0.09 e^- on N and 0.03 e^- on O) in their ground singlet state indicating the presence of weak antiferromagnetic coupling.

The molecular orbital treatment on complex **2** in the quintet state shows that the singly occupied molecular orbitals (SOMOs) are not significantly delocalized which is also evident from the weak ferromagnetic interaction (Fig. 13). In SOMO and SOMO-1 most of the orbital contributions are localized on the periphery of the molecule instead of in the magnetic core. But in SOMO-2 and SOMO-3 the orbital contribution comes mostly from the core, and the oxygen in the oxo-bridge contributes a significant population, reflecting the strong ferromagnetic interaction through it. Due to the planar geometry of the molecule, the $d_{x^2-y^2}$ orbital of the Cu^{II} atoms interacts with the bridging atoms in σ fashion. The out-of-phase interactions of π* type MOs localized on the –N–O– bridges (SOMO-2 and SOMO-3) with the appropriate symmetry-adapted combinations of the $d_{x^2-y^2}$ orbital of the four Cu^{II} magnetic centers supporting the antiferromagnetic coupling nature of this bridge.

The frontier orbitals of **3** in both the spin states indicated a dominant contribution from the Cu^{II} centers. Very small contributions of the oximato –N–O– bridges indicated weak antiferromagnetic exchange interaction through these bridges (ESI, Fig. S8†).

Conclusions

In conclusion, we have successfully synthesized a series of polynuclear transition metal complexes using 2-pyrimidineamidoxime, to illustrate its potential to act as a neutral blocking donor (complex **1**), but more interestingly the opportunities that it offers when it acts as both a monoanionic and a dianionic bridging ligand in the same complex (**2** and **3**). At room temperature a Cu^{II} one-dimensional chain was obtained, but at high temperature (under solvothermal conditions) we were able to isolate two new collapsed 12-MC-4 complexes. In the heterometallic 12-MC-4 (**3**), Ni^{II} centers preferentially occupied the square planar environment rather than a square pyramidal geometry. The crystal packing of all the complexes revealed 2D (**1** and **2**) and 3D (**3**) networks construction *via* H-bonding interactions. The temperature dependent magnetic susceptibility data of **2** shows weak ferromagnetic interaction. The competitive magnetic interactions between Cu^{II} atoms through the ferromagnetic oxo-bridge and the antiferromagnetic –N–O– pathway lead to the resultant weak ferromagnetic interaction. The variable temperature magnetic susceptibility of **3** reveals the presence of weak antiferromagnetic interaction through –N–O– bridges. The DFT calculations were performed in broken symmetry formalism and the results are in good agreement with the experimental observations.

Acknowledgements

S. M. is grateful to the Council for Scientific and Industrial Research, India, for research fellowship. Authors are thankful to Prof. S. V. Bhat for EPR experiments and Arun Kumar Bar for his support in structure refinements. Authors also thank the Department of Science and Technology (DST), New Delhi for financial support.

References

1 (*a*) G. Mezei, C. M. Zaleski and V. L. Pecoraro, *Chem. Rev.*, 2007, **107**, 4933; (*b*) V. L. Pecoraro, A. J. Stemmler, B. R. Gibney, J. J. Bodwin, H. Wang, J. W. Kampf and A. Barwinski, *Progress in Inorganic Chemistry*, K. D. Karlin, Ed.; Wiley: New York, 1997; Vol. 45, pp 83-177; (*c*) M. S. Lah and V. L. Pecoraro, *Comments Inorg. Chem.*, 1990, **11**, 59; (*d*) V. L. Pecoraro, *Inorg. Chim. Acta*, 1989, **155**, 171; (*e*) M. S. Lah and V. L. Pecoraro, *J. Am. Chem. Soc.*, 1989, **111**, 7258; (*f*) J. J. Bodwin and V. L. Pecoraro, *Inorg. Chem.*, 2000, **39**, 3434; (*g*) M. Moon, I. Kim and M. S. Lah, *Inorg. Chem.*, 2000, **39**, 2710; (*h*) H. Piotrowski, K. Polborn, G. Hilt and K. Severin, *J. Am. Chem. Soc.*, 2001, **123**, 2699; (*i*) R. Beckett and B. F. Hoskins, *J. Chem. Soc., Dalton Trans.*, 1972, 291; (*j*) R. J. Butcher, C. J. O'Connor and E. Sinn, *Inorg. Chem.*, 1981, **20**, 537; (*k*) W. Uhl, J. Molter and B. Neumuller, *Chem.–Eur. J.*, 2001, **7**, 4216; (*l*) X. Yang, Z. Zheng, C. B. Knobler and M. F. Hawthorne, *J. Am. Chem. Soc.*, 1993, **115**, 193; (*m*) H. Chen, M. F. Maestre and R. H. Fish, *J. Am. Chem. Soc.*, 1995, **117**, 3631; (*n*) B. Chaudret, B. Delavaux and R. Poilblanc, *Coord. Chem. Rev.*, 1988, **86**, 191; (*o*) J. Xiao and R. J. Puddephatt, *Coord. Chem. Rev.*, 1995, **143**, 457.

2 (*a*) J.-M. Lehn, *Supramolecular Chemistry, concepts and perspectives*, VCH: New York, 1995; (*b*) J.-M. Lehn, *Angew. Chem., Int. Ed. Engl.*, 1990, **29**, 1304; (*c*) S. R. Seidel and P. J. Stang, *Acc. Chem. Res.*, 2002, **35**, 972; (*d*) D. Philp and J. F. Stoddart, *Angew. Chem., Int. Ed. Engl.*, 1996, **35**, 1154; (*e*) M. Fujita, J. Y. Kwon, S. Washizu and K. Ogura, *J. Am. Chem. Soc.*, 1994, **116**, 1151; (*f*) S. Leininger, B. Olenyuk and P. J. Stang, *Chem. Rev.*, 2000, **100**, 853; (*g*) T. Yamamoto, A. M. Arif and P. J. Stang, *J. Am. Chem. Soc.*, 2003, **125**, 12309.

3 (*a*) V. L. Pecoraro, A. J. Stemmler, B. R. Gibney, J. J. Bodwin, H. Wang, J. W. Kampf and A. Barwins-Ki, *Prog. Inorg. Chem.*, 1996, **45**, 83; (*b*) G. Mezei, C. M. Zaleski and V. L. Pecoraro, *Chem. Rev.*, 2007, **107**, 4933.

4 (*a*) R. W. Saalfrank, N. Löw, F. Hampel and H.-D. Stachel, *Angew. Chem., Int. Ed. Engl.*, 1996, **35**, 2209; (*b*) H. Chen, M. F. Maestre and R. H. Fish, *J. Am. Chem. Soc.*, 1995, **117**, 3631; (*c*) H. Chen, S. Ogo and R. H. Fish, *J. Am. Chem. Soc.*, 1996, **118**, 4993.

5 (*a*) M. Casarin, C. Corvaja, C. di Nicola, D. Falcomer, L. Franco, M. Monari, L. Pandolfo, C. Pettinari, F. Piccinelli and P. Tagliatesta, *Inorg. Chem.*, 2004, **43**, 5865; (*b*) G. A. Ardizzoia, S. Cenini, G. La Monica, N. Masciocchi and M. Moret, *Inorg. Chem.*, 1994, **33**, 1458; (*c*) A. Maspero, S. Brenna, S. Galli and A. Penoni, *J. Organomet. Chem.*, 2003, **672**, 123; (*d*) G. A. Ardizzoia, M. A. Angaroni, G. La Monica, F. Cariati, S. Cenini, M. Moret and N. Masciocchi, *Inorg. Chem.*, 1991, **30**, 4347.

6 (*a*) K. Severin, *Coord. Chem. Rev.*, 2003, **245**, 3; (*b*) H. Piotrowski, K. Polborn, G. Hilt and K. Severin, *J. Am. Chem. Soc.*, 2001, **123**, 2699; (*c*) H. Piotrowski, G. Hilt, A. Schulz, P. Mayer, K. Polborn and K. Severin, *Chem.–Eur. J.*, 2001, **7**, 3196; (*d*) H. Piotrowski and K. Severin, *Proc. Natl. Acad. Sci. U. S. A.*, 2002, **99**, 4997; (*e*) Z. Grote, M.-L. Lehaire, R. Scopelliti and K. Severin, *J. Am. Chem. Soc.*, 2003, **125**, 13638; (*f*) Z. Grote, R. Scopelliti and K. Severin, *Angew. Chem., Int. Ed.*, 2003, **42**, 3821; (*g*) Z. Grote, R. Scopelliti and K. Severin, *J. Am. Chem. Soc.*, 2004, **126**, 16959.

7 A. D. Cutland, R. G. Malkani, J. W. Kampf and V. L. Pecoraro, *Angew. Chem., Int. Ed.*, 2000, **39**, 2689.

8 (*a*) A. C. Cutland-Van Noord, J. W. Kampf and V. L. Pecoraro, *Angew. Chem., Int. Ed.*, 2002, **41**, 4667; (*b*) J. J. Bodwin and V. L. Pecoraro, *Inorg. Chem.*, 2000, **39**, 3434; (*c*) D. Moon, J. Song, B. J. Kim, B. J. Suh and M. S. Lah, *Inorg. Chem.*, 2004, **43**, 8230; (*d*) D. Moon and M. S. Lah, *Inorg. Chem.*, 2005, **44**, 1934; (*e*) R. Wang, M. Hong, J. Luo, R. Cao and J. Weng, *Chem. Commun.*, 2003, 1018; (*f*) V. L. Pecoraro, J. J. Bodwin and A. D. Cutland, *J. Solid State Chem.*, 2000, **152**, 68; (*g*) J. J. Bodwin, A. D. Cutland, R. G. Malkani and V. L. Pecoraro, *Coord. Chem. Rev.*, 2001, **216–217**, 489; (*h*) R. J. Butcher, G. Diven, G. Erickson, G. M. Mockler and E. Sinn, *Inorg. Chim. Acta*, 1986, **123**, L17.

9 (*a*) T. Lis, *Acta Crystallogr., Sect. B: Struct. Crystallogr. Cryst. Chem.*, 1980, **B36**, 2042; (*b*) R. Sessoli, D. Gatteschi and M. A. Novak, *Nature*, 1993, **365**, 141; (*c*) R. Sessoli, H. Tsai, A. R. Schake, S. Wang, J. B. Vincent, K. Folting, D. Gatteschi, G. Christou and D. N. Hendrickson, *J. Am. Chem. Soc.*, 1993, **115**, 1804; (*d*) A. L. Barra, L. Brunel, D. Gatteschi, L. Pardi and R. Sessoli, *Acc. Chem. Res.*, 1998, **31**, 460; (*e*) G. Christou, D. Gatteschi, D. N. Hendrickson and R. Sessoli, *MRS Bull.*, 2000, **25**, 66; (*f*) D. Gatteschi, R. Sessoli and A. Cornia, *Chem. Commun.*, 2000, 725; (*g*) D. Gatteschi and R. Sessoli, *Angew. Chem., Int. Ed.*, 2003, **42**, 268; (*h*) R. E. P. Winpenny, Ed. *Single-Molecule Magnets and Related Phenomena (Structure and Bonding)* Springer: New York, 2006; Vol. 122; (*i*) S. L. Tripp, R. E. Dunin-Borkowski and A. Wei, *Angew. Chem., Int. Ed.*, 2003, **42**, 5591; (*j*) W. S. Seo, H. H. Jo, K. Lee, B. Kim, S. J. Oh and J. T. Park, *Angew. Chem., Int. Ed.*, 2004, **43**, 1115; (*k*) J. Park, E. Lee, N.-M. Hwang, M. Kang, S. C. Kim, Y. Hwang, J.-G. Park, H.-J. Noh, J.-Y. Kim, J.-H. Park and T. Hyeon, *Angew. Chem., Int. Ed.*, 2005, **44**, 2872; (*l*) J. Lai, K. V. P. M. Shafi, A. Ulman, K. Loos, R. Popovitz-Biro, Y. Lee, T. Vogt and C. Estournes, *J. Am. Chem. Soc.*, 2005, **127**, 5730; (*m*) S. Karasawa, G. Zhou, H. Morikawa and N. Koga, *J. Am. Chem. Soc.*, 2003, **125**, 13676; (*n*) V. Chandrasekhar, B. M. Pandian, R. Azhakar, J. J. Vittal and R. Clerac, *Inorg. Chem.*, 2007, **46**, 5140; (*o*) H. Oshio, M. Nihei, S. Koizumi, T. Shiga, H. Nojiri, H. Nakano, N. Shirakawa and M. Akatsu, *J. Am. Chem. Soc.*, 2005, **127**, 4568; (*p*) S. Wang, J.-L. Zuo, H.-C. Zhou, H. J. Choi, Y. Ke, J. R. Long and X.-Z. You, *Angew. Chem., Int. Ed.*, 2004, **43**, 5940; (*q*) Y. Song, P. Zhang, X.-M. Ren, X.-F. Shen, Y.-Z. Li and X.-Z. You, *J. Am. Chem. Soc.*, 2005, **127**, 3708; (*r*) N. Ishikawa, M. Sugita, T. Ishikawa, S. Koshihara and Y. Kaizu, *J. Am. Chem. Soc.*, 2003, **125**, 8694; (*s*) E. K. Brechin, *Chem. Commun.*, 2005, 5141; (*t*) D. Foguet-Albiol, T. A. O'Brien, W. Wernsdorfer, B. Moulton, M. J. Zaworotko, K. A. Abboud and G. Christou, *Angew. Chem., Int. Ed.*, 2005, **44**, 897.

10 (*a*) C. Dendrinou-Samara, G. Psomas, L. Iordanidis, V. Tangoulis and D. P. Kessissoglou, *Chem.–Eur. J.*, 2001, **7**, 5041; (*b*) C. Dendrinou-Samara, L. Alevizopoulou, L. Iordanidis, E. Samaras and D. P. Kessissoglou, *J. Inorg. Biochem.*, 2002, **89**, 89.

11 G. Psomas, C. Dendrinou-Samara, M. Alexiou, A. Tsohos, C. P. Raptopoulou, A. Terzis and D. P. Kessissoglou, *Inorg. Chem.*, 1998, **37**, 6556.

12 (*a*) A. J. Stemmler, A. Barwinski, M. J. Baldwin, V. Young and V. L. Pecoraro, *J. Am. Chem. Soc.*, 1996, **118**, 11962; (*b*) M. Careri, F. Dallavalle, M. Tegoni and I. Zagnoni, *J. Inorg. Biochem.*, 2003, **93**, 174.

13 (*a*) M. S. Lah, M. L. Kirk, W. Hatfield and V. L. Pecoraro, *J. Chem. Soc., Chem. Commun.*, 1989, 1606; (*b*) A. D. Cutland, J. A. Halfen, J. W. Kampf and V. L. Pecoraro, *J. Am. Chem. Soc.*, 2001, **123**, 6211; (*c*) M. Tegoni, F. Dallavalle, B. Belosi and M. Remelli, *Dalton Trans.*, 2004, 1329; (*d*) B. R. Gibney, D. P. Kessissoglou, J. W. Kampf and V. L. Pecoraro, *Inorg. Chem.*, 1994, **33**, 4840; (*e*) C. Dendrnou-samara, C. M. Zaleski, A. Evagorou, J. W. Kampf, V. L. Pecoraro and D. P. Kessissoglou, *Chem. Commun.*, 2003, 2668.

14 (*a*) M. Alexiou, C. Dendrinou-Samara, C. P. Raptopoulou, A. Terzis and D. P. Kessissoglou, *Inorg. Chem.*, 2002, **41**, 4732; (*b*) A. J. Stemmler, J. W. Kampf and V. L. Pecoraro, *Inorg. Chem.*, 1995, **34**, 2271; (*c*) J. L. Song, J. G. Mao, H. Y. Zeng, R. K. Kremer and Z. C. Dong, *Inorg. Chem. Commun.*, 2003, **6**, 891.

15 (*a*) B. Li, D. D. Han, G. Z. Cheng and Z. P. Ji, *Inorg. Chem. Commun.*, 2005, **8**, 216; (*b*) S. Lin, S. X. Liu, J. Q. Huang and C. C. Lin, *J. Chem. Soc., Dalton Trans.*, 2002, 1595; (*c*) R. P. John, K. Lee and M. S. Lah, *Chem. Commun.*, 2004, 2660; (*d*) B. Kwak, H. Rhee, S. Park and M. S. Lah, *Inorg. Chem.*, 1998, **37**, 3599; (*e*) B. Kwak, H. Rhee and M. S. Lah, *Polyhedron*, 2000, **19**, 1985; (*f*) S. Lin, S. X. Liu and B. Z. Lin, *Wuji Huaxue Xuebao*, 2002, **18**, 1205; (*g*) S. Lin, S. X. Liu and B. Z. Lin, *Inorg. Chim. Acta*, 2002, **328**, 69; (*h*) J. Song, D. Moon and M. S. Lah, *Bull. Korean Chem. Soc.*, 2002, **23**, 708; (*i*) D. Moon, K. Lee, R. P. John, G. H. Kim, B. J. Suh and M. S. Lah, *Inorg. Chem.*, 2006, **45**, 7991; (*j*) K. Lee, R. P. John, M. Park, D. Moon, H.-C. Ri, G. H. Kim and M. S. Lah, *Dalton Trans.*, 2008, 131; (*k*) X. Liu, W. Liu, K. Lee, M. Park, H.-C. Ri, G. H. Kim and M. S. Lah, *Dalton Trans.*, 2008, 6579; (*l*) R. P. John, K. Lee, B. J. Kim, B. J. Suh, H. Rhee and M. S. Lah, *Inorg. Chem.*, 2005, **44**, 7109; (*m*) W. Liu, K. Lee, M. Park, R. P. John, D. Moon, Y. Zou, X. Liu, H.-C. Ri, G. H. Kim and M. S. Lah, *Inorg. Chem.*, 2008, **47**, 8807.

16 (*a*) R. A. Coxall, S. G. Harris, D. K. Henderson, S. Parsons, P. A. Tasker and R. E. P. Winpenny, *J. Chem. Soc., Dalton Trans.*, 2000, 2349; (*b*) G. Psomas, A. J. Stemmler, C. Dendrinou-Samara, J. J. Bodwin, M. Schneider, M. Alexiou, J. W. Kampf, D. P. Kessissoglou and V. L. Pecoraro, *Inorg. Chem.*, 2001, **40**, 1562.

17 Th. C. Stamatatos, S. Dionyssopoulou, P. Kyritsis, C. P. Raptopoulou, A. Terzis, R. Vicente, A. Escuer and S. P. Perlepes, *Inorg. Chem.*, 2005, **44**, 3374.

18 (*a*) M. Orama, H. Saarinen and J. Korvenranta, *Acta Chem. Scand.*, 1994, **48**, 127; (*b*) J. A. Bertrand, J. H. Smith and D. G. VanDer Veer, *Inorg. Chem.*, 1977, **16**, 1477; (*c*) H. Saarinen, M. Orama, T. Raikas and J. Korvenranta, *Acta Chem. Scand., Ser. A*, 1986, **40a**, 396; (*d*) H. Saarinen, M. Orama and J. Korvenranta, *Acta Chem. Scand.*, 1989, **43**, 834; (*e*) G. Psomas, A. J. Stemmler, C. Dendrinou-Samara, J. J. Bodwin, M. Scheider, M. Alexiou, J. W. Kampf, D. P. Kessissoglou and V. L. Pecoraro, *Inorg. Chem.*, 2001, **40**, 1562.

19 (*a*) C. M. Zaleski, E. C. Depperman, J. W. Kampf, M. L. Kirk and V. L. Pecoraro, *Inorg. Chem.*, 2006, **45**, 10022; (*b*) E. Rumberger, L. N. Zakharov, A. L. Rheingold and D. N. Hendrickson, *Inorg. Chem.*, 2004, **43**, 6531; (*c*) E. M. Rumberger, S. J. Shah, C. C. Beedle, L. N. Zakharov, A. L. Rheingold and D. N. Hendrickson, *Inorg. Chem.*, 2005, **44**, 2742; (*d*) M. Murugesu, J. Raftery, W. Wernsdorfer, G. Christou and E. K. Brechin, *Inorg. Chem.*, 2004, **43**, 4203; (*e*) C. Cadiou, M. Murrie, C. Paulsen, V. Villar, W. Wernsdorfer and R. E. P. Winpenny, *Chem. Commun.*, 2001, 2666; (*f*) H. Andres, R. Basler, A. J. Blake, C. Cadiou, G. Chaboussant, C. M. Grant, H. Gudel, M. Murrie, S. Parsons, C. Paulsen, F. Semadini, V. Villar, W. Wernsdorfer and R. E. P. Winpenny, *Chem.–Eur. J.*, 2002, **8**, 4867; (*g*) A. Mishra, W. Wernsdorfer, K. A. Abboud and G. Christou, *J. Am. Chem. Soc.*, 2004, **126**, 15648; (*h*) N. Ishikawa, M. Sugita and W. Wernsdorfer, *J. Am. Chem. Soc.*, 2005, **127**, 3650; (*i*) N. Ishikawa, S. Otsuka and Y. Kaizu, *Angew. Chem., Int. Ed.*, 2005, **44**, 731.

20 C. Papatriantafyllopoulou, L. F. Jones, T. D. Nguyen, N. Matamoros-Salvador, L. Cunha-Silva, F. A. A. Paz, J. Rocha, M. Evangelisti, E. K. Brechin and S. P. Perlepes, *Dalton Trans.*, 2008, 3153.

21 (*a*) R. L. Dutta, and A. Syamal, *Elements of Magnetochemistry*, 2nd ed.; East West Press: Manhattan Beach, CA, 1993; (*b*) O. Kahn, *Molecular Magnetism*, VCH publisher: New York, 1993.

22 P. V. Fish, G. A. Allan, S. Bailey, J. Blagg, R. G. Butt, M. G. Collis, D. Greiling, K. James, J. Kendall, A. McElroy, D. McCleverty, C. Reed, R. Webster and G. A. Whitlock, *J. Med. Chem.*, 2007, **50**, 3442.

23 *SMART/SAINT* Bruker AXS, Inc.: Madison, WI (2004).

24 G. M. Sheldrick, *SHELX-97, Program for the Solution and Refinement of Crystal Structures* University of Göttingen, Göttingen, Germany (1998).

25 L. J. Farrugia, *WinGX: An integrated system of windows programs for the solution, refinement and analysis for single crystal X-ray*

diffraction data, version 1.65.04; Department of Chemistry: University of Glasgow, 2003. (L. J. Farrago, *J. Appl. Crystallogr.*, 1999, **32**, 837).
26 G. M. Sheldrick, *SADABS, Bruker nonius area detector scaling and absorption correction*, version 2.05; University of Göttingen, Göttingen, Germany (1999).
27 L. J. Farrugia, *J. Appl. Crystallogr.*, 1997, **30**, 565.
28 A. L. Spek, *Acta Crystallogr., Sect. A: Found. Crystallogr.*, 1990, **46**, 34.
29 (*a*) E. Ruiz, P. Alemany, S. Alvarez and J. Cano, *J. Am. Chem. Soc.*, 1997, **119**, 1297; (*b*) E. Ruiz, A. Rodríguez-Fortea, J. Cano, S. Alvarez and P. Alemany, *J. Comput. Chem.*, 2003, **24**, 982; (*c*) E. Ruiz, J. Cano, S. Alvarez and P. Alemany, *J. Comput. Chem.*, 1999, **20**, 1391; (*d*) E. Ruiz, *Struct. Bonding*, 2004, **113**, 71.
30 A. D. Becke, *J. Chem. Phys.*, 1993, **98**, 5648.
31 M. J. Frisch, G. W. Trucks, H. B. Schlegel, G. E. Scuseria, M. A. Robb, J. R. Cheeseman, J. A. Montgomery, Jr., T. Vreven, K. N. Kudin, J. C. Burant, J. M. Millam, S. S. Iyengar, J. Tomasi, V. Barone, B. Mennucci, M. Cossi, G. Scalmani, N. Rega, G. A. Petersson, H. Nakatsuji, M. Hada, M. Ehara, K. Toyota, R. Fukuda, J. Hasegawa, M. Ishida, T. Nakajima, Y. Honda, O. Kitao, H. Nakai, M. Klene, X. Li, J. E. Knox, H. P. Hratchian, J. B. Cross, V. Bakken, C. Adamo, J. Jaramillo, R. Gomperts, R. E. Stratmann, O. Yazyev, A. J. Austin, R. Cammi, C. Pomelli, J. Ochterski, P. Y. Ayala, K. Morokuma, G. A. Voth, P. Salvador, J. J. Dannenberg, V. G. Zakrzewski, S. Dapprich, A. D. Daniels, M. C. Strain, O. Farkas, D. K. Malick, A. D. Rabuck, K. Raghavachari, J. B. Foresman, J. V. Ortiz, Q. Cui, A. G. Baboul, S. Clifford, J. Cioslowski, B. B. Stefanov, G. Liu, A. Liashenko, P. Piskorz, I. Komaromi, R. L. Martin, D. J. Fox, T. Keith, M. A. Al-Laham, C. Y. Peng, A. Nanayakkara, M. Challacombe, P. M. W. Gill, B. G. Johnson, W. Chen, M. W. Wong, C. Gonzalez and J. A. Pople, *GAUSSIAN 03 (Revision C.02)*, Gaussian, Inc., Wallingford, CT, 2004.
32 C. Lee, W. Yang and R. G. Parr, *Phys. Rev. B: Condens. Matter*, 1988, **37**, 785.
33 E. Ruiz, S. Alvarez, J. Cano and V. Polo, *J. Chem. Phys.*, 2005, **123**, 164110.
34 A. Kotani and H. Ogasawarab, *J. Electron Spectrosc. Relat. Phenom.*, 1992, **60**, 257.
35 K. Kambe, *J. Phys. Soc. Jpn.*, 1950, **5**, 48.
36 T. Afrati, C. Dendrinou-Samara, C. Raptopoulou, A. Terzis, V. Tangoulis, A. Tsipis and D. P. Kessissoglou, *Inorg. Chem.*, 2008, **47**, 7545.
37 E. Ruiz, J. Cano, S. Alvarez and P. Alemany, *J. Am. Chem. Soc.*, 1998, **120**, 11122.

